[6]D. F. Jackson and V. K. Kembhavi, Phys. Rev. 178, 1626 (1969); D. F. Jackson, Phys. Letters 32B, 233 (1970).
[7]A. M. Bernstein and W. A. Seidler, Phys. Letters 34B, 569 (1971); and to be published. See also Bernstein, Ref. 1d.
[8]B. Tatischeff and I. Brissaud, Nucl. Phys. A155, 89 (1970).
[9]A. Dar and Z. Kirzon, Phys. Letters 37B, 166 (1971).
[10]R. J. Glauber, in *Lectures in Theoretical Physics* (Interscience, New York, 1959), Vol. I.
[11]N. Austern, Ann. Phys. (N.Y.) 15, 299 (1961).
[12]J. A. Wheeler, Phys. Rev. 99, 630 (1955).
[13]W. H. Miller, J. Chem. Phys. 51, 3631 (1969).
[14]G. Wollmer, Z. Physik 226, 423 (1969).
[15]W. G. Rich *et al.*, Phys. Rev. A 4, 2253 (1971).
[16]P. C. Sabatier, Nuovo Cimento 37, 1180 (1965).
[17]M. H. Simbel and A. Y. Abul-Magd, Z. Physik 238, 321 (1970).
[18]D. A. Sparrow, private communication.
[19]R. G. Newton, *Scattering Theory of Waves and Particles* (McGraw-Hill, New York, 1966).
[20]The exact integration of the Schrödinger equation is carried out using a version of the optical-model code ABACUS written by E. Auerbach with the appropriate modifications due to T. Provost.
[21]A. Martin, *Scattering Theory: Unitarity, Analyticity and Crossing* (Springer-Verlag, Berlin, 1969), p. 8.
[22]W. A. Seidler, Ph.D. thesis, Massachusetts Institute of Technology, 1972 (unpublished).
[23]R. P. Marchi and C. R. Mueller, J. Chem. Phys. 38, 740 (1963).

PHYSICAL REVIEW C VOLUME 6, NUMBER 3 SEPTEMBER 1972

Semileptonic Weak Interactions with C^{12}†

J. S. O'Connell*
National Bureau of Standards, Washington, D. C. 20234
and
T. W. Donnelly and J. D. Walecka
Institute of Theoretical Physics, Department of Physics, Stanford University, Stanford, California 94305
(Received 3 May 1972)

A unified analysis of semileptonic weak and electromagnetic interactions in nuclei is applied to the $A=12$ system. The particle-hole model is used to describe the nuclear dynamics of B^{12}, C^{12}, and N^{12}. Neutrino reaction cross sections are presented for comparison with future experiments.

I. INTRODUCTION

A unified discussion of semileptonic weak interactions in nuclei: neutrino reactions, charged-lepton capture, and β decay, has recently been presented[1] in close analogy to the theory of electron scattering.[2] The topic of semileptonic weak interactions in nuclei is of interest for two reasons. First, most of the fundamental tests of our ideas on weak interactions have involved nuclei, and if nuclei are to serve as laboratories with which to conduct experiments on weak interactions, it is essential that the nuclear physics of these processes be well understood. Second, once the fundamental nature of the weak interactions is understood it can be used as a known probe for testing our theoretical ideas on nuclear structure and for exciting new and unusual states in nuclei. The electromagnetic interaction in electron scattering also plays such a role and because of the close analogy between the processes, it is important to discuss semileptonic weak processes and electron scattering together. In fact, the conserved-vector-current (CVC) theory states that half the matrix elements in the weak processes, those coming from the vector current are *identical* to those measured in electron scattering. In addition, electron scattering data at all $\vec{q}^2$ provide a test of the nuclear wave functions, allowing us to have some confidence in predictions for new processes, and serving in many cases to eliminate nuclear physics uncertainties in examining the basic structure of the weak interaction itself. The weak interactions are, in principle, a richer source of information on nuclear structure because of the interaction of the leptons with the axial-vector current, as well as the vector current in the target.

Donnelly *et al.*[3] and Donnelly[4] have recently presented a detailed comparison of the predictions of

the particle-hole model for the $T=1$ states in C^{12} with experimental large-angle inelastic electron scattering results. Donnelly computed the particle-hole interaction from a nonsingular Serber-Yukawa two-nucleon potential fit to low-energy nucleon-nucleon scattering and took the unperturbed particle-hole configuration energies from neighboring nuclei. Harmonic-oscillator single-particle wave functions were used with an oscillator parameter determined from elastic electron scattering. This particle-hole model is extremely successful in predicting the location of the states, generally to better than 1 MeV and in predicting the inelastic form factors out to momentum transfers as large as $|\vec{q}| \approx 700$ MeV. The calculated amplitudes in this simple model, however, are too large by a factor of the order of $\sqrt{2}$ for the negative-parity oscillations and about 2 for the positive-parity doublet. In this paper we use the particle-hole configuration-mixed wave functions of Donnelly to compute the semileptonic weak processes in C^{12}. The computed matrix elements are then normalized by the factors found in the comparison to the measured electron scattering form factors of these states. We present some theoretical arguments for this procedure.

There is one discrete transition for which all the weak (except neutrino) and electromagnetic processes have been measured and that is the $0^+ \rightleftarrows 1^+$ transition in the B^{12}-C^{12}-N^{12} multiplet and we discuss this case in some detail.

There has been a great deal of theoretical work done on weak interactions in C^{12}. An extensive review of this work is contained in Ref. 1, and we shall not attempt to repeat all the references here. We would just point out that no one has carried out a single, unified calculation of all the semileptonic processes involving a single nucleus and fully brought detailed inelastic electron scattering data to bear on the weak processes. In addition, neutrino excitation of the high-spin particle-hole states, which actually dominates the neutrino cross section to discrete levels at high energies, has never been considered.

In Section II the main results of Ref. 1 are reviewed. Section III contains a detailed discussion of the results for C^{12} and Sec. IV is the conclusion. An appendix relating neutrino cross sections with those for inelastic electron scattering within the framework of certain assumptions is also included.

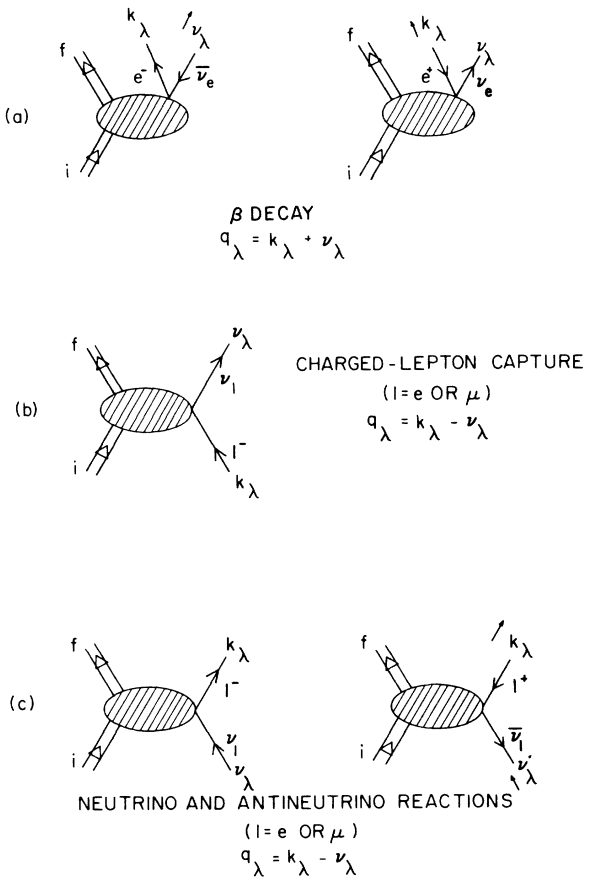

FIG. 1. (a)–(c) Semileptonic weak processes. The four-momentum transfer $q_\lambda = (\vec{q}, -i\omega)$ is given in terms of the lepton four-momentum $k_\lambda = (\vec{k}, i\epsilon)$ and the neutrino four-momentum $\nu_\lambda = (\vec{\nu}, i\nu)$.

II. FORMALISM

The semileptonic weak processes to be considered here are shown in Fig. 1.[5] If we denote the weak Hamiltonian which contains the interaction between the leptons and the nuclear systems by $\hat{H}_W$, then we may use first-order perturbation theory to obtain the reaction rates between discrete nuclear levels. For β decay from nuclear state $|i\rangle$ to state $|f\rangle$ [Fig. 1(a)] we obtain the reaction rate[1]

$$d\omega_\beta = (2\pi)^{-5} V^2 k\epsilon (W_0 - \epsilon)^2 \, d\epsilon \int d\Omega_\nu \int d\Omega_k \times \sum_{\substack{\text{lepton} \\ \text{spins}}} \frac{1}{2J_i + 1} \sum_{M_i M_f} |\langle f|\hat{H}_W|i\rangle|^2, \quad (1)$$

where the kinematics are defined in Fig. 1(a) ($k = |\vec{k}|$ here), W_0 is the maximum electron energy (including rest mass), and V is a normalization volume. The full differential rate has been integrated over neutrino and electron solid angles Ω_ν and Ω_k, respectively, and the summations are over all magnetic quantum numbers, since no polarizations are measured. From this β spectrum

we can obtain the total decay rate:

$$\omega_\beta = \int_{m_e}^{W_0} \left(\frac{d\omega_\beta}{d\epsilon}\right) d\epsilon , \tag{2}$$

where m_e is the electron mass. The second weak process we consider is muon capture shown in Fig. 1(b). For the capture rate again using first-order perturbation theory one obtains[1]

$$\omega_\mu = (2\pi)^{-1} V^2 \nu^2 \sum_{\substack{\text{lepton}\\ \text{spins}}} \frac{1}{2J_i+1} \sum_{M_i M_f} |\langle f|\hat{H}_W|i\rangle|^2 , \tag{3}$$

where the kinematic variables are defined in the figure. Finally the neutrino reactions are shown in Fig. 1(c). These proceed with differential cross sections[1]

$$\frac{d\sigma_\nu}{d\Omega} = (2\pi)^{-2} V^2 k\epsilon \sum_{\substack{\text{lepton}\\ \text{spins}}} \frac{1}{2J_i+1} \sum_{M_i M_f} |\langle f|\hat{H}_W|i\rangle|^2 , \tag{4}$$

where $k = |\vec{k}|$ or expressing this in terms of the variable $\vec{q}^2$

$$\frac{d\sigma_\nu}{d\vec{q}^2} = \tfrac{1}{2}(2\pi)^{-1} V^2 \frac{\epsilon}{\nu} \sum_{\substack{\text{lepton}\\ \text{spins}}} \frac{1}{2J_i+1} \sum_{M_i M_f} |\langle f|\hat{H}_W|i\rangle|^2 . \tag{5}$$

In all cases nuclear recoil has been neglected, but will be included later.

These processes involve matrix elements of the weak-interaction Hamiltonian $\hat{H}_W$. To obtain a form for this operator we can first consider the interaction of leptons with hadrons as expressed by the current-current interaction

$$\mathcal{H}_W(\vec{x}) = -\frac{G}{\sqrt{2}} g_\lambda^{(+)} g_\lambda^{(-)} , \tag{6}$$

where

$$\begin{aligned} g_\lambda^{(-)} &= g_\lambda^{(-)}(\text{hadronic}) + j_\lambda^{(-)}(\text{leptonic}) , \\ g_\lambda^{(+)} &= (\vec{g}^{(-)\dagger}, i g_0^{(-)\dagger}) , \end{aligned} \tag{7}$$

with coupling constant G given by[1] $GM_p^2 = 1.023 \pm 0.002 \times 10^{-5}$, where M_p = proton mass. The leptonic part of the current is given by

$$j_\lambda^{(-)}(\text{leptonic}) = i[\bar{\psi}_e \gamma_\lambda(1+\gamma_5)\psi_{\nu_e} + \bar{\psi}_\mu \gamma_\lambda(1+\gamma_5)\psi_{\nu_\mu}] , \tag{8}$$

where ψ, $\bar{\psi}$ are the relativistic quantum fields describing the leptons. The Hamiltonian we require for the semileptonic weak processes in Eqs. (1), (3), and (4) is given by

$$\hat{H}_W = -\frac{G}{\sqrt{2}} \int d\vec{x}\, \hat{g}_\lambda(\vec{x}) j_\lambda(\vec{x}) ; \tag{9}$$

or using the four momentum q_λ defined in Fig. 1 for the various processes and denoting the leptonic matrix element by $l_\lambda e^{-i\vec{q}\cdot\vec{x}}$, we require the nuclear matrix elements of the Hamiltonian

$$\langle f|\hat{H}_W|i\rangle = -\frac{G}{\sqrt{2}} l_\lambda \int d\vec{x}\, e^{-i\vec{q}\cdot\vec{x}} \langle f|\hat{g}_\lambda(\vec{x})|i\rangle \tag{10}$$

involving the Fourier transform of the hadronic current-density matrix elements. The only assumptions we will make at this point are that there exists a local current-density operator $\hat{g}_\lambda(\vec{x})$ for the target (this could, for example, include meson-exchange-current contributions) and that the target is sufficiently well localized in space that partial integrations on the transition matrix elements $\langle f|\hat{g}_\lambda(\vec{x})|i\rangle \equiv [g_\lambda(\vec{x})]_{fi}$, discarding the vanishingly small contributions at infinity, may be carried out at will. We also assume that the initial and final states of the target are characterized by definite angular momentum and parity, J^π, and neglect target recoil in the transition matrix elements.

The same procedure as employed in studying electromagnetic interactions which involve only the vector current density is then followed; that is, a multipole analysis is performed on the hadronic-current matrix elements yielding the following expression[1]

$$\begin{aligned} \frac{1}{2J_i+1} \sum_{M_i M_f} |\langle f|\hat{H}_W|i\rangle|^2 = \frac{G^2}{2} \frac{1}{2J_i+1} \Big\{ &\sum_{\lambda=\pm1} l_\lambda l_\lambda^* \sum_{J=1}^{\infty} 2\pi |\langle J_f \| \hat{T}_J^{\text{el}} + \lambda \hat{T}_J^{\text{mag}} \| J_i\rangle|^2 \\ &+ \sum_{J=0}^{\infty} 4\pi [l_3 l_3^* |\langle J_f \| \hat{\mathfrak{L}}_J \| J_i\rangle|^2 + l_0 l_0^* |\langle J_f \| \hat{\mathfrak{M}}_J \| J_i\rangle|^2 \\ &- 2\mathrm{Re} l_3 l_0^* \langle J_f \| \hat{\mathfrak{L}}_J \| J_i\rangle \langle J_f \| \hat{\mathfrak{M}}_J \| J_i\rangle^*] \Big\} , \end{aligned} \tag{11}$$

where the appropriate lepton traces are listed in Tables I and II.

If we assume that the excited states in the $A(Z, N)$ nucleus involved in electron scattering are the isobaric analogs of states in the $A(Z \pm 1, N \mp 1)$ nuclei reached in the weak processes considered here, then the matrix elements differ only in their isospin dependence: $\frac{1}{2}\tau_3$ for the electromagnetic isovector operators

TABLE I. Lepton matrix elements and sign factors in lepton traces.

Process	Vl_λ	S_1	S_2	S_1S_2	S_3
β^- decay$(e^-\bar{\nu}_e)$	$\bar{u}(\vec{k})\gamma_\lambda(1+\gamma_5)v(-\vec{\nu})$	−1	−1	+1	$\mathrm{sgn}(\epsilon-\nu)$
β^+ decay$(e^+\nu_e)$	$\bar{u}(\vec{\nu})\gamma_\lambda(1+\gamma_5)v(-\vec{k})$	+1	−1	−1	$\mathrm{sgn}(\epsilon-\nu)$
Charged-lepton capture$(\mu^-\nu_\mu)$, $(e^-\nu_e)$	$\bar{u}(\vec{\nu})\gamma_\lambda(1+\gamma_5)u(\vec{k})$	+1	−1	−1	−1
Neutrino reactions$(\nu_l l^-)$	$\bar{u}(\vec{k})\gamma_\lambda(1+\gamma_5)u(\vec{\nu})$	−1	+1	−1	+1
Antineutrino reactions$(\bar{\nu}_l l^+)$	$\bar{v}(-\vec{\nu})\gamma_\lambda(1+\gamma_5)v(-\vec{k})$	+1	+1	+1	+1

and $\tau_\pm = \mp(\tau_1 \pm i\tau_2)/2$ for the weak operators. The matrix elements are related by the identity

$$\left|\langle T+1, M_T = T|\sum_i \tfrac{1}{2}\tau_3(i)\,\mathcal{O}(i)|\,T, M_T = T\rangle\right|^2 = \frac{1}{2(T+1)}\left|\langle T+1, M_T = T\pm 1|\sum_i \tau_\pm(i)\,\mathcal{O}(i)|\,T, M_T = T\rangle\right|^2, \tag{12}$$

where the sum is over nucleons and $\mathcal{O}(i)$ is any one of the multipole operators in first quantization.

The multipole operators involved above are given in terms of the hadronic current and in terms of the functions (involving spherical Bessel functions, spherical harmonics, and vector spherical harmonics)[1,2]

$$M_J^M(\vec{x}) \equiv j_J(\kappa x)Y_J^M(\Omega_x)\,, \tag{13}$$

$$\vec{M}_{JL}^M(\vec{x}) \equiv j_L(\kappa x)\vec{Y}_{JL1}^M(\Omega_x)\,, \tag{14}$$

where $\kappa = |\vec{q}|$. The operators then are

$$\hat{\mathfrak{M}}_{JM} \equiv \hat{M}_{JM} + \hat{M}^5_{JM} \equiv \int d\vec{x}\, M_J^M(\vec{x})\,\hat{\mathcal{J}}_0(\vec{x})\,, \tag{15}$$

$$\hat{\mathfrak{L}}_{JM} \equiv \hat{L}_{JM} + \hat{L}^5_{JM} \equiv i\int d\vec{x}\left(\frac{1}{\kappa}\vec{\nabla}M_J^M(\vec{x})\right)\cdot\hat{\vec{\mathcal{J}}}(\vec{x})\,. \tag{16}$$

$$\hat{\mathfrak{T}}^{\mathrm{el}}_{JM} \equiv \hat{T}^{\mathrm{el}}_{JM} + \hat{T}^{\mathrm{el}5}_{JM} \equiv i\int d\vec{x}\left(\frac{1}{\kappa}\vec{\nabla}\times\vec{M}_{JJ}^M(\vec{x})\right)\cdot\hat{\vec{\mathcal{J}}}(\vec{x})\,, \tag{17}$$

$$\hat{\mathfrak{T}}^{\mathrm{mag}}_{JM} \equiv \hat{T}^{\mathrm{mag}}_{JM} + \hat{T}^{\mathrm{mag}5}_{JM} \equiv \int d\vec{x}\,\vec{M}_{JJ}^M(\vec{x})\cdot\hat{\vec{\mathcal{J}}}(\vec{x})\,, \tag{18}$$

namely, the Coulomb, longitudinal, transverse electric, and transverse magnetic multipole operators, each containing a vector part and an axial-vector part (denoted by 5) coming from the respective combinations of the current density

$$\hat{\mathcal{J}}_\lambda(\mathrm{hadronic}) = \hat{J}_\lambda + \hat{J}_{\lambda 5}\,. \tag{19}$$

The rates for the weak processes we are interested in here can now be written in terms of nuclear ma-

TABLE II. Lepton traces: $\frac{1}{2}\nu^2\sum_{\text{lepton spins}}$. Here $\hat{\nu} = \vec{\nu}/|\vec{\nu}|$, $\hat{q} = \vec{q}/|\vec{q}|$, $\vec{k} = \epsilon\vec{\beta}$ and $\beta = |\vec{\beta}|$.

Summand	General result	Threshold $\beta \to 0$	ERL $\beta \to 1$
$\frac{1}{2}(\vec{l}\cdot\vec{l}^* - l_3 l_3^*)$	$1-(\hat{\nu}\cdot\hat{q})(\vec{\beta}\cdot\hat{q})$	1	$\frac{q_\lambda^2}{\vec{q}^2}\cos^2(\frac{1}{2}\theta)+2\sin^2(\frac{1}{2}\theta)$
$l_0 l_0^*$	$1+\hat{\nu}\cdot\vec{\beta}$	1	$2\cos^2(\frac{1}{2}\theta)$
$l_3 l_3^*$	$1-\hat{\nu}\cdot\vec{\beta}+2(\hat{\nu}\cdot\hat{q})(\vec{\beta}\cdot\hat{q})$	1	$\frac{\omega^2}{\vec{q}^2}\cdot 2\cos^2(\frac{1}{2}\theta)$
$-l_3 l_0^*$	$-\hat{q}\cdot(\hat{\nu}+\vec{\beta})$	S_2	$+\frac{\omega}{\lvert\vec{q}\rvert}\cdot 2\cos^2(\frac{1}{2}\theta)$
$-\frac{i}{2}(\vec{l}\times\vec{l}^*)_3$	$-S_1\hat{q}\cdot(\hat{\nu}-\vec{\beta})$	S_1S_2	$2\sin(\frac{1}{2}\theta)\left(\frac{q_\lambda^2}{\vec{q}^2}\cos^2(\frac{1}{2}\theta)+\sin^2(\frac{1}{2}\theta)\right)^{1/2}S_1S_3$

trix elements of these multipole operators. For β decay we get[1]

$$d\omega_{\beta^\mp} = \frac{2}{\pi^2} G^2 \beta \epsilon^2 (W_0^\mp - \epsilon)^2 d\epsilon \int \frac{d\Omega_\nu}{4\pi} \int \frac{d\Omega_k}{4\pi} \frac{1}{2J_i+1}$$
$$\times F^\mp(Z,\epsilon) \Bigg(\sum_{J=0}^{\infty} \{ (1+\hat{\nu}\cdot\vec{\beta}) |\langle J_f \| \hat{\mathfrak{M}}_J \| J_i \rangle|^2 + [1-\hat{\nu}\cdot\vec{\beta}+2(\hat{\nu}\cdot\hat{q})(\hat{q}\cdot\vec{\beta})] |\langle J_f \| \hat{\mathfrak{L}}_J \| J_i \rangle|^2$$
$$- \hat{q}\cdot(\hat{\nu}+\vec{\beta}) 2\,\mathrm{Re}\langle J_f \| \hat{\mathfrak{L}}_J \| J_i \rangle \langle J_f \| \hat{\mathfrak{M}}_J \| J_i \rangle^* \}$$
$$+ \sum_{J=1}^{\infty} \{ [1-(\hat{\nu}\cdot\hat{q})(\hat{q}\cdot\vec{\beta})] (|\langle J_f \| \hat{\mathcal{T}}_J^{\mathrm{el}} \| J_i \rangle|^2 + |\langle J_f \| \hat{\mathcal{T}}_J^{\mathrm{mag}} \| J_i \rangle|^2)$$
$$\pm \hat{q}\cdot(\hat{\nu}-\vec{\beta}) 2\,\mathrm{Re}\langle J_f \| \hat{\mathcal{T}}_J^{\mathrm{mag}} \| J_i \rangle \langle J_f \| \hat{\mathcal{T}}_J^{\mathrm{el}} \| J_i \rangle^* \} \Bigg). \tag{20}$$

Here $\vec{k} = \epsilon\vec{\beta}$, $\hat{\nu} = \vec{\nu}/|\vec{\nu}|$, $\hat{q} = \vec{q}/|\vec{q}|$, W_0 is the maximum $e^\mp$ energy, and $F^\mp(Z,\epsilon)$ is a factor which takes into account the distortion of the electron wave function by the Coulomb field of the daughter nucleus of charge Z and is given[1] approximately by

$$F^\mp(Z,\epsilon) \simeq 2\pi\eta^\mp / (e^{2\pi\eta^\mp} - 1), \tag{21}$$

where $\eta^\mp = \mp Z\alpha/\beta$, $\beta = |\vec{\beta}|$, and α is the fine-structure constant. The reduced matrix elements are evaluated at momentum transfer $\kappa = |\vec{q}|$.

For muon capture from the $1s$ Bohr atomic orbit (where we may treat the muons nonrelativistically) we obtain for the decay rate[1]

$$\omega_\mu = \frac{2G^2\nu^2}{1+\nu/M_T} |\phi_{1s}|^2_{\mathrm{av}} \frac{1}{2J_i+1} \left(\sum_{J=0}^{\infty} |\langle J_f \| \hat{\mathfrak{M}}_J - \hat{\mathfrak{L}}_J \| J_i \rangle|^2 + \sum_{J=1}^{\infty} |\langle J_f \| \hat{\mathcal{T}}_J^{\mathrm{el}} - \hat{\mathcal{T}}_J^{\mathrm{mag}} \| J_i \rangle|^2 \right), \tag{22}$$

where a phase-space factor $(1+\nu/M_T)^{-1}$ accounting for nuclear recoil has now been included and $|\phi_{1s}|^2_{\mathrm{av}}$ is the muon atomic wave function averaged over the volume of the nucleus given by

$$|\phi_{1s}|^2_{\mathrm{av}} = R\,|\phi^0_{1s}(0)|^2 = \frac{R}{\pi} \left(\frac{m_\mu M_T}{m_\mu + M_T} Z\alpha \right)^3, \tag{23}$$

with m_μ the muon mass, M_T the target mass, and R a reduction factor taking into account the finite extent of the nuclear charge distributions (= 0.86 for C^{12}, see Ref. 1). The neutrino energy ν at which the multipole operators are evaluated is determined from energy conservation using the atomic binding energy and the initial and final nuclear energies.

Finally the neutrino and antineutrino reaction cross sections can be similarly obtained and are given by[1]

$$\left(\frac{d\sigma_\nu}{d\vec{q}^2} \right)_{\substack{\nu \\ \bar{\nu}}} = G^2 \frac{\epsilon}{\nu} \frac{1}{2J_i+1} \Bigg(\sum_{J=0}^{\infty} \{ (1+\hat{\nu}\cdot\vec{\beta}) |\langle J_f \| \hat{\mathfrak{M}}_J \| J_i \rangle|^2 + [1-\hat{\nu}\cdot\vec{\beta}+2(\hat{\nu}\cdot\hat{q})(\hat{q}\cdot\vec{\beta})] |\langle J_f \| \hat{\mathfrak{L}}_J \| J_i \rangle|^2$$
$$- \hat{q}\cdot(\hat{\nu}+\vec{\beta}) 2\,\mathrm{Re}\langle J_f \| \hat{\mathfrak{L}}_J \| J_i \rangle \langle J_f \| \hat{\mathfrak{M}}_J \| J_i \rangle^* \}$$
$$+ \sum_{J=1}^{\infty} \{ [1-(\hat{\nu}\cdot\hat{q})(\hat{q}\cdot\vec{\beta})] (|\langle J_f \| \hat{\mathcal{T}}_J^{\mathrm{el}} \| J_i \rangle|^2 + |\langle J_f \| \hat{\mathcal{T}}_J^{\mathrm{mag}} \| J_i \rangle|^2$$
$$\pm \hat{q}\cdot(\hat{\nu}-\vec{\beta}) 2\,\mathrm{Re}\langle J_f \| \hat{\mathcal{T}}_J^{\mathrm{mag}} \| J_i \rangle \langle J_f \| \hat{\mathcal{T}}_J^{\mathrm{el}} \| J_i \rangle^* \} \Bigg), \tag{24}$$

with the reduced matrix elements of the multipole operators being evaluated at momentum transfer $\kappa = |\vec{q}|$. This formula correctly includes nuclear recoil in the density of final states. In the extreme relativistic limit (ERL) when $\beta = 1$ we obtain

$$\left(\frac{d\sigma_\nu}{d\vec{q}^2} \right)^{\mathrm{ERL}}_{\substack{\nu \\ \bar{\nu}}} = 2G^2 \frac{\epsilon}{\nu} \frac{1}{2J_i+1} \cos^2(\tfrac{1}{2}\theta) \Bigg\{ \sum_{J=0}^{\infty} |\langle J_f \| \hat{\mathfrak{M}}_J + \frac{\omega}{|\vec{q}|} \hat{\mathfrak{L}}_J \| J_i \rangle|^2 + \left[\frac{1}{2} \frac{q_\lambda^2}{\vec{q}^2} + \tan^2(\tfrac{1}{2}\theta) \right]$$
$$\times \sum_{J=1}^{\infty} [|\langle J_f \| \hat{\mathcal{T}}_J^{\mathrm{el}} \| J_i \rangle|^2 + |\langle J_f \| \hat{\mathcal{T}}_J^{\mathrm{mag}} \| J_i \rangle|^2] \mp \tan(\tfrac{1}{2}\theta) \left[\frac{q_\lambda^2}{\vec{q}^2} + \tan^2(\tfrac{1}{2}\theta) \right]^{1/2}$$
$$\times \sum_{J=1}^{\infty} 2\,\mathrm{Re}\langle J_f \| \hat{\mathcal{T}}_J^{\mathrm{mag}} \| J_i \rangle \langle J_f \| \hat{\mathcal{T}}_J^{\mathrm{el}} \| J_i \rangle^* \Bigg\}, \tag{25}$$

where $\hat{\nu}\cdot\vec{\beta}/\beta = \cos\theta$. This result can be directly compared with the corresponding formula for inelastic electron scattering. (See Refs. 1 and 2 and the Appendix.)

To proceed further, we need a prescription for obtaining the nuclear weak current density. We first observe that the matrix elements of the current between *nucleon* states of momenta $\vec{p}$ and $\vec{p}'$ may be written using Lorentz covariance and isospin invariance as

$$\langle \vec{p}' | J_\lambda^{(-)} | \vec{p} \rangle = \frac{i}{V}\bar{u}(\vec{p}')[F_1\gamma_\lambda + F_2\sigma_{\lambda\lambda'}q_{\lambda'} + iF_S q_\lambda]\tau_- u(\vec{p}), \tag{26}$$

$$\langle \vec{p}' | J_{\lambda 5}^{(-)} | \vec{p} \rangle = \frac{i}{V}\bar{u}(\vec{p}')[F_A\gamma_5\gamma_\lambda - iF_P\gamma_5 q_\lambda - F_T\gamma_5\sigma_{\lambda\lambda'}q_{\lambda'}]\tau_- u(\vec{p}), \tag{27}$$

where $u(\vec{p})$, $\bar{u}(\vec{p}')$ are Dirac spinors for the nucleon. These form factors are all functions of four-momentum transfer $q_\lambda{}^2 = (p-p')_\lambda{}^2$. Beyond this general current-current theory one can consider a more restrictive theory obtained by making the CVC hypothesis, in which case one can identify the vector coupling constants $F_{1,2}$ with their electromagnetic counterparts $F_{1,2}^V$:

$$F_{1,2} = F_{1,2}^V, \tag{28}$$

$$F_1^V(0) = 1, \tag{29}$$

$$F_1^V(0) + 2M_N F_2^V(0) = \mu^V(0) = 4.706, \tag{30}$$

where M_N is the nucleon mass. For the other coupling constants we use

$$F_A^\beta(0) = F_A^\mu(0) = -1.23 \pm 0.01, \tag{31}$$

from studies of neutron β decay and of the ratio $(\pi \to e+\nu)/(\pi \to \mu+\nu)$, and for the pseudoscalar coupling constant we assume pion-pole dominance and use the Goldberger-Treiman relation to obtain

$$F_P(q_\lambda{}^2) = \frac{2M_N F_A(q_\lambda{}^2)}{q_\lambda{}^2 + m_\pi{}^2}, \tag{32}$$

where m_π is the pion mass. The coupling constants $F_1^V(q_\lambda{}^2)$, $\mu^V(q_\lambda{}^2)$, and $F_A(q_\lambda{}^2)$ are all assumed to have the momentum dependence of the nucleon charge form factor, namely $[1+q_\lambda{}^2/(855\ \mathrm{MeV})^2]^{-2}$, whereas $F_P(q_\lambda{}^2)$ has the momentum dependence implied by Eq. (32). See Ref. 1 for a more complete discussion of the coupling constants including further references. In addition, if the true hadronic current has the same parity, charge-conjugation, time-reversal, and isospin-transformation properties as the $V-A$ current made of bare nucleons, then the second-class currents vanish, that is $F_S = F_T = 0$. We shall assume CVC and omit the second-class currents in all of the following formalism.

Having a form for the interaction Hamiltonian between the lepton current and the current for individual nucleons we moreover make the assumption that the second-quantized nuclear-current-density operator is given by

$$\hat{\mathcal{J}}_\lambda(0) = \sum_{\vec{p}'\sigma'\rho'}\sum_{\vec{p}\sigma\rho} a_{\vec{p}'\sigma'\rho'}^\dagger \langle \vec{p}'\sigma'\rho' | \mathcal{J}_\lambda(0) | \vec{p}\sigma\rho\rangle a_{\vec{p}\sigma\rho}, \tag{33}$$

where $\{\vec{p}\sigma\rho\}$ are a complete set of momentum, spin, and isospin quantum numbers for a nucleon, a and $a^\dagger$ are annihilation and creation operators in the nuclear Hilbert space, and the matrix element is taken to be the single-nucleon expression given in Eqs. (26) and (27). In using this prescription we have (i) assumed that the nucleon coordinates provide a complete description of the nuclear many-body system and so have neglected meson-exchange currents; and (ii) used matrix elements evaluated for free particles (on-mass-shell), whereas we expect some small modifications when the nucleons are bound in a nucleus.

For most discrete transitions of interest, the interesting $\vec{q}^2$ region is determined by the *nuclear* form factors and the motion of the nucleons in the target can be treated nonrelativistically. The single-nucleon amplitudes in Eqs. (26) and (27) can then be reduced through order $|\vec{p}|/M_N \simeq (v/c)_{\text{nucleons}}$ by writing the Dirac wave functions as

$$u(\vec{p}\lambda) \simeq \begin{pmatrix} \chi_\lambda \\ \dfrac{\vec{\sigma}\cdot\vec{p}}{2M_N}\chi_\lambda \end{pmatrix}, \tag{34}$$

where χ_λ is a two-component Pauli spinor. This is carried out in detail in Ref. 1. We shall only give the results here. The single-particle multipole operators required in studying these weak or electromagnetic processes can be given in terms of the basic nuclear multipole operators we can form. They include four vector operators (note we have used current conservation in the second line),

$$M_{JM}(\vec{x}) = F_1^V M_J^M(\vec{x}), \tag{35}$$

$$L_{JM}(\vec{x}) = -\frac{\omega}{\kappa}F_1^V M_J^M(\vec{x}), \tag{36}$$

$$T_{JM}^{\mathrm{el}}(\vec{x}) = \frac{\kappa}{M_N}[F_1^V \Delta_J'^M(\vec{x}) + \tfrac{1}{2}\mu^V \Sigma_J^M(\vec{x})], \tag{37}$$

$$iT^{\mathrm{mag}}_{JM}(\vec{x}) = \frac{K}{M_N}\left[F_1^V \Delta^M_J(\vec{x}) - \tfrac{1}{2}\mu^V \Sigma'^M_J(\vec{x})\right], \tag{38}$$

and four axial-vector operators,

$$iM^5_{JM}(\vec{x}) = \frac{K}{M_N}\left[F_A \Omega^M_J(\vec{x}) + \tfrac{1}{2}(F_A - \lambda M_N F_P)\Sigma''^M_J(\vec{x})\right], \tag{39}$$

$$-iL^5_{JM}(\vec{x}) = \left[F_A - \tfrac{1}{2}\lambda'\left(\frac{K}{M_N}\right)^2 M_N F_P\right]\Sigma'^M_J(\vec{x}), \tag{40}$$

$$-iT^{\mathrm{el}5}_{JM}(\vec{x}) = F_A \Sigma'^M_J(\vec{x}), \tag{41}$$

$$T^{\mathrm{mag}5}_{JM}(\vec{x}) = F_A \Sigma^M_J(\vec{x}). \tag{42}$$

Here M_N is the nucleon mass, $\lambda = m_\mu/M_N$ for muon capture, $\lambda = \omega/M_N$ for the neutrino processes and $\lambda = m_e/M_N \simeq 0$ for all electron processes. The parameter $\lambda' = 0$ except in the neutrino processes, where $\lambda' = 1$. The multipoles in Eqs. (35)–(37) and (42) have parity $(-)^J$, whereas the rest have parity $(-)^{J+1}$. There are only seven fundamental single-particle operators that enter and they are

$$M^M_J(\vec{x}), \tag{43}$$

$$\Delta^M_J(\vec{x}) \equiv \vec{M}^M_{JJ}(\vec{x}) \cdot \frac{1}{K}\vec{\nabla}, \tag{44}$$

$$\Delta'^M_J(\vec{x}) \equiv -i\left[\frac{1}{K}\vec{\nabla}\times\vec{M}^M_{JJ}(\vec{x})\right]\cdot\frac{1}{K}\vec{\nabla},$$
$$= \left[-\left(\frac{J}{2J+1}\right)^{1/2}\vec{M}^M_{JJ+1}(\vec{x}) + \left(\frac{J+1}{2J+1}\right)^{1/2}\vec{M}^M_{JJ-1}(\vec{x})\right]\cdot\frac{1}{K}\vec{\nabla}, \tag{45}$$

$$\Sigma^M_J(\vec{x}) \equiv \vec{M}^M_{JJ}(\vec{x})\cdot\vec{\sigma}, \tag{46}$$

$$\Sigma'^M_J(\vec{x}) \equiv -i\left[\frac{1}{K}\vec{\nabla}\times\vec{M}^M_{JJ}(\vec{x})\right]\cdot\vec{\sigma}$$
$$= \left[-\left(\frac{J}{2J+1}\right)^{1/2}\vec{M}^M_{JJ+1}(\vec{x}) + \left(\frac{J+1}{2J+1}\right)^{1/2}\vec{M}^M_{JJ-1}(\vec{x})\right]\cdot\vec{\sigma}, \tag{47}$$

$$\Sigma''^M_J(\vec{x}) \equiv \left[\frac{1}{K}\vec{\nabla}M^M_J(\vec{x})\right]\cdot\vec{\sigma}$$
$$= \left[\left(\frac{J+1}{2J+1}\right)^{1/2}\vec{M}^M_{JJ+1}(\vec{x}) + \left(\frac{J}{2J+1}\right)^{1/2}\vec{M}^M_{JJ-1}(\vec{x})\right]\cdot\vec{\sigma}, \tag{48}$$

and

$$\Omega^M_J(\vec{x}) \equiv M^M_J(\vec{x})\vec{\sigma}\cdot\frac{1}{K}\vec{\nabla}. \tag{49}$$

Expressions for the single-particle reduced matrix elements of all of these operators have been given previously,[1,2] excepting the last which yields

$$\langle n'l'\tfrac{1}{2}j' \| \Omega_J \| nl\tfrac{1}{2}j\rangle = (-)^{l'}\left[\frac{(2j'+1)(2j+1)(2l'+1)(2J+1)}{4\pi}\right]^{1/2}$$
$$\times\left[-\delta_{j,l+1/2}\sqrt{2l+3}\begin{Bmatrix} J & l' & l+1 \\ \frac{1}{2} & j & j' \end{Bmatrix}\begin{pmatrix} l' & J & l+1 \\ 0 & 0 & 0 \end{pmatrix}\left\langle n'l'\left| j_J(\rho)\left(\frac{d}{d\rho} - \frac{l}{\rho}\right)\right| nl\right\rangle\right.$$
$$\left. + \delta_{j,l-1/2}\sqrt{2l-1}\begin{Bmatrix} J & l' & l-1 \\ \frac{1}{2} & j & j' \end{Bmatrix}\begin{pmatrix} l' & J & l-1 \\ 0 & 0 & 0 \end{pmatrix}\left\langle n'l'\left| j_J(\rho)\left(\frac{d}{d\rho} + \frac{l+1}{\rho}\right)\right| nl\right\rangle\right], \tag{50}$$

where $\rho = \kappa x$. In this expression

$$\langle n'l'|\, j_J(\rho)\,|nl\rangle = \int_0^\infty x^2 dx\, R^*_{n'l'}(x)\, j_J(\kappa x) R_{nl}(x), \tag{51}$$

with $R_{nl}(x)$ the normalized radial wave functions. Analytic expressions for these matrix elements when the radial wave functions are obtained using an infinite harmonic-oscillator potential have been given elsewhere.[2]

The final connection with nuclear physics is made by using second-quantized transition multipole operators in the nuclear many-particle Hilbert space:

$$\hat{T}_{JM} = \sum_{\alpha\beta} c^\dagger_\alpha \langle \alpha | T_{JM} | \beta\rangle c_\beta, \tag{52}$$

where T_{JM} is any one of the first-quantized operators given in Eqs. (35)–(42). The matrix elements and creation and annihilation operators $c^\dagger$, c bear single-particle labels α, β. The reduced matrix elements $\langle J_f \| \hat{T}_J \| J_i\rangle$ can then be evaluated once a specific model is assumed for the initial and final nuclear states. For the many-body nuclear system we shall employ shell-model wave functions which are not translationally invariant and give rise to a center-of-mass correction.[2] For

the special case of harmonic-oscillator wave functions, used throughout this work, this entails multiplying all matrix elements by $e^{y/A}$, where $y = (\frac{1}{2}b\kappa)^2$ and A is the nuclear mass number. In the next section we shall consider the mass-12 system in detail treating these nuclear excited states in the Tamm-Dancoff approximation (TDA) as single-particle-hole states.

III. RESULTS AND DISCUSSION

In this section we present detailed results for the mass-12 system B^{12}, C^{12}, and N^{12} obtained within the framework of the single-particle-hole model. The ground state of C^{12} with $J^\pi T = 0^+ 0$ is treated as a closed $1p_{3/2}$ shell. The low-lying $T = 1$ excited states of C^{12} are taken as linear combinations of the even-parity $(1p_{1/2})(1p_{3/2})^{-1}$ or odd-parity $(1d_{5/2})(1p_{3/2})^{-1}$, $(2s_{1/2})(1p_{3/2})^{-1}$, $(1d_{3/2})(1p_{3/2})^{-1}$, $(1p_{1/2})(1s_{1/2})^{-1}$ single-particle-hole states combined to form a specific $J^\pi T$:

$$|E, J^\pi T; M_J M_T\rangle = \sum_K \psi^K_{E, J^\pi T} \hat{A}^{K\dagger}_{J^\pi T; M_J M_T} |0\rangle . \quad (53)$$

Here $|0\rangle$ is the closed-shell ground state, $\psi^K_{E, J^\pi T}$ are the admixture amplitudes, and the particle-hole creation operators are given by

$$\hat{A}^{K\dagger}_{J^\pi T; M_J M_T} = \sum_{m_j m_{j'}} \sum_{m_t m_{t'}} \langle j m_j j' m_{j'} | j j' J M_J \rangle \times \langle \tfrac{1}{2} m_t \tfrac{1}{2} m_{t'} | \tfrac{1}{2} \tfrac{1}{2} T M_T \rangle a^\dagger_\alpha b^\dagger_{\alpha'} , \quad (54)$$

where α and α' represent the set of single-particle quantum numbers $\{nl\frac{1}{2}jm_j; \frac{1}{2}m_t\}$ and K stands for the quantum numbers identifying the pure particle-hole pair, $a = \{nlj\}$ for the particle, $a' = \{n'l'j'\}$ for the hole. The admixture amplitudes $\psi^K_{E, J^\pi T}$ in the TDA are determined by diagonalizing the Hamiltonian. In the present work we use the TDA amplitudes determined in previous electron scattering studies of C^{12}, where a Serber-Yukawa interaction with parameters adjusted to fit low-energy nucleon-nucleon scattering was employed.[3,4] The energy eigenvalues E obtained in this calculation are in quite good agreement with experiment, usually within an MeV of the experimental value and this model provides an excellent description of the entire inelastic electron scattering spectrum to $T = 1$ states of C^{12} up to about 30-MeV excitation energy. The other states needed in the present work, that is the ground and excited states of B^{12} and N^{12}, are treated as isobaric analog states of these $T = 1$ particle-hole states in C^{12}. For example, the ground states of B^{12} and N^{12} are both taken to have the same wave functions as the 1^+1 state in C^{12} which occurs experimentally at 15.11 MeV. The point of view taken in considering this isobaric multiplet is to consider all pieces of the current on an equal footing. Since the electron scattering form factor is the best determined experimentally, we use it to fix the oscillator parameter and the amplitude reduction factor and then use these unchanged in discussing the weak processes. In fact, electron scattering only yields information about the vector part of the current and perhaps a closer comparison exists among the weak processes themselves, for example between β decay and muon capture. However, the fact that all the calculated results are in good agreement with experiment with the same parameters strongly suggests that the particle-hole model may be used in the present manner as a vehicle to relate all these processes to each other.

It is then straightforward to calculate the doubly reduced matrix elements of any one-body operator (in the present context any one of the transition multipole operators in Sec. II):

$$\langle E, J^\pi T :: \hat{T}_{J^\pi T} :: 0\rangle = \sum_K \psi^K_{E, J^\pi T} \langle a :: T_{J^\pi T} :: a' \rangle , \quad (55)$$

[recall $K \equiv a(a')^{-1}$] that is, we have a linear combination of single-particle matrix elements weighted with the admixture amplitudes.

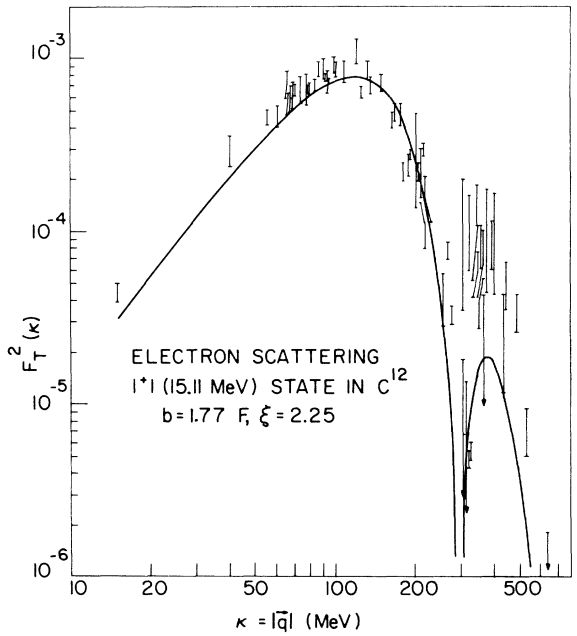

FIG. 2. Inelastic electron scattering form factor $F_T^2(\kappa)$ [see Eq. (A3)] as a function of $\kappa = |\vec{q}|$ for the 1^+1 state at 15.11 MeV in C^{12}. The curve is a best fit with b and ξ as adjustable parameters. References to the data are given in a previous study of electron scattering (see Ref. 6). The photon point at $\kappa = \omega$ is given in the figure but has not been used in fitting the curve.

We have at this point left open the possibility of there being two remaining free parameters: the oscillator parameter $b=(M_N\omega_0)^{-1/2}$ and an effective over-all reduction of all admixture amplitudes by a scale factor

$$\psi^K_{E,J^\pi T}\rightarrow\frac{1}{\xi}\psi^K_{E,J^\pi T}. \tag{56}$$

In past studies of electron scattering[3,4] the oscillator parameter has been fixed by requiring that the C^{12} elastic electron scattering form factor have its diffraction minimum at the correct experimental momentum transfer and that the calculated Coulomb energy differences agree with experiment. These both suggest a value of $b=1.64$ F. In studying all of the states except the 1^+1 state we will consistently use this value, so that in fact the oscillator parameter is not really a free parameter in the present work. In Sec. III A, where we study the 1^+1 state alone and try to do a more accurate calculation, we will vary the oscillator parameter slightly to obtain the best over-all fit with the 1^+1 *inelastic* electron scattering form factor and then use this value in the weak interaction calculations. However, in Sec. III B where all of the particle-hole states are considered together we will use the value $b=1.64$ F for everything.

The reduction factor ξ is not really an arbitrary parameter either. Recent studies[6] of C^{12} in which the ground state was taken to involve particles in both $1p_{3/2}$ and $1p_{1/2}$ shells (intermediate coupling[7]) show that for electron scattering the dominant effect is to scale the form factor in amplitude but leave largely unchanged the momentum transfer dependence. A preliminary investigation of the $0^+0\rightarrow 1^+1$ weak processes indicate that the factor ξ can be essentially explained by the opening of the p shell. Here we continue to use the TDA and show how excellent agreement among all the electromagnetic and weak processes can be obtained

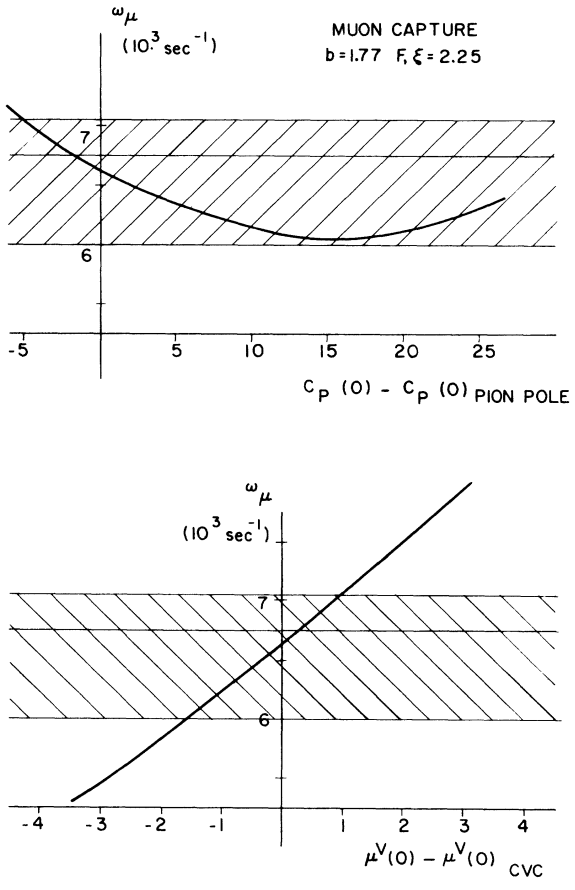

FIG. 3. Muon-capture rate as a function of the coupling constants $\mu^V(0)$ and $C_P\equiv m_\mu F_P/F_A$. The values used throughout the present work are $\mu^V(0)_{\text{CVC}}=4.706$ and $C_P(0)_{\text{pion pole}}=10.18$. The value of the latter frequently quoted is $C_P\equiv C_P(0)m_\pi{}^2/(q_\lambda{}^2+m_\pi{}^2)$, where $q_\lambda{}^2$ is appropriate to μ capture on a proton, $C_P=6.72$. The shaded regions correspond to the experimental capture rate (see E. J. Maier, R. M. Edelstein, and R. T. Siegel, Phys. Rev. 133, B663 (1964)].

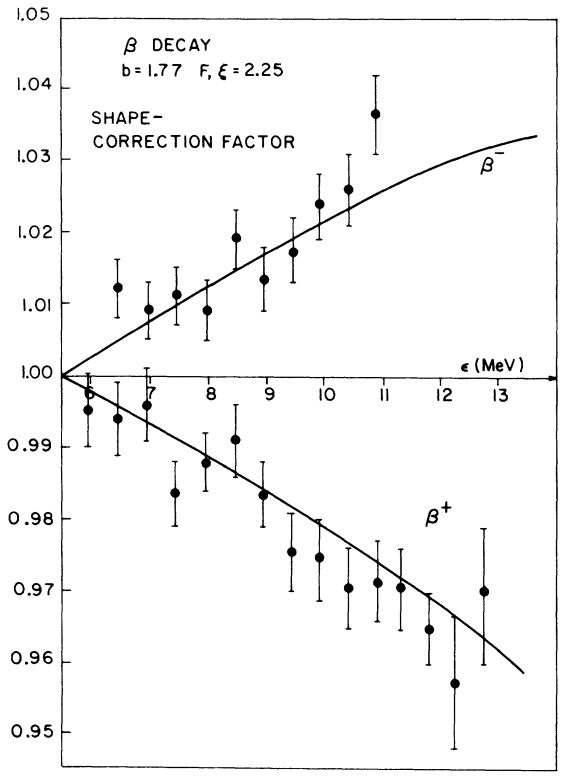

FIG. 4. Shape-correction factor in β decay defined as $(d\omega^\pm_\beta/d\epsilon)\times[G^2\beta\epsilon^2(W^\pm_0-\epsilon)^2]^{-1}$. In accordance with the data from Ref. 9 the curves are normalized to unity at electron energy $\epsilon=5.45$ MeV.

once the parameter ξ is fixed by any one of them. Since the electron scattering form factors are the best determined experimentally, we use these data to determine ξ in our study of the $0^+0 \leftrightarrow 1^+1$ transitions in the next subsection.

A. $0^+0 \leftrightarrow 1^+1$ Transitions in Mass 12

The reactions studied here involve the 0^+0 ground state of C^{12}, the 1^+1 excited state at 15.11 MeV in C^{12}, and 1^+1 ground states of B^{12} and N^{12}; they are the following:

$$e^- + C^{12} \rightarrow C^{12*} + e^{-\prime}, \tag{57a}$$

$$C^{12*} \rightarrow C^{12} + \gamma, \tag{57b}$$

$$B^{12} \rightarrow C^{12} + e^- + \bar{\nu}_e, \tag{57c}$$

$$N^{12} \rightarrow C^{12} + e^+ + \nu_e, \tag{57d}$$

$$\mu^- + C^{12} \rightarrow B^{12} + \nu_\mu, \tag{57e}$$

$$\nu_l + C^{12} \rightarrow N^{12} + l^-, \quad l = e \text{ or } \mu. \tag{57f}$$

The first two involve only the vector current, while the remaining involve both vector and axial-vector currents. With TDA as our basic assumption for the wave functions, so that the 0^+0 ground state is a closed $1p_{3/2}$ shell and the 1^+1 states are pure $(1p_{1/2})(1p_{3/2})^{-1}$ in nature, we obtain the following for the reduced matrix elements of the necessary multipole operators

$$\langle p_{1/2} \| \Delta_1 \| p_{3/2} \rangle = \frac{1}{\sqrt{4\pi}} \frac{\sqrt{2}}{3} e^{-y}, \tag{58}$$

$$\langle p_{1/2} \| \Sigma_1' \| p_{3/2} \rangle = \frac{1}{\sqrt{4\pi}} \frac{4\sqrt{2}}{3} (1 - \tfrac{1}{2} y) e^{-y}, \tag{59}$$

$$\langle p_{1/2} \| \Sigma_1'' \| p_{3/2} \rangle = \frac{1}{\sqrt{4\pi}} \frac{4}{3} (1 - y) e^{-y}, \tag{60}$$

$$\langle p_{1/2} \| \Omega_1 \| p_{3/2} \rangle = -\frac{1}{\sqrt{4\pi}} \frac{5}{3} (1 - \tfrac{2}{5} y) e^{-y}. \tag{61}$$

Here $y = (\frac{1}{2} b\kappa)^2$. To fix the oscillator parameter b and the reduction factor ξ we compare the electron scattering form factor [reaction (57a)] with experiment in Fig. 2. The best χ^2 fit was obtained with $b = 1.77$ F and $\xi = 2.25$, that is with a reduction in the inelastic electron scattering cross section by $(2.25)^2$. Calculations using the particle-hole states obtained in the open-shell random-phase approximation (RPA)[6] suggest that the form factor here may not be completely due to the 1^+1 contribution, but may also have contributions from nearby $T = 0$ states. In particular these calculations indicate that a nearby 2^-0 state yields a form factor which is small at low momentum transfer, but rises at high momentum transfer to increase the net form factor for $\kappa \sim 300$–400 MeV and produce better agreement with experiment. Since the experimental error bars are generally large at high momentum transfer, the χ^2 fit is not changed significantly by ignoring all but the 1^+1 state. This determines the isovector matrix element of the electromagnetic current and by CVC gives us the vector current contributions in the weak processes. The dominant operator in this electromagnetic transition is the spin multipole Σ_1'' [Eq. (47)]. The spin multipoles are also the dominant operators in the axial-vector current. We therefore assume here, as is true within the framework of an RPA[1] or more complete shell-model[6] calculation, that the same model will apply to the axial-vector-current matrix elements, that is, that there is an over-all reduction factor due to the use of the TDA wave functions which becomes completely unnecessary with the use of better wave functions. The results are then given in Table III. Here we have used the value $b = 1.77$ F and in comparing with experiment for the measured reactions have given the reduction factors required in each case. It is very encouraging that the agreement is so good: With $\xi = 2.25$ as determined by electron scattering, the results for all these reaction rates are in essential agreement with experiment.

If we confine our attention to the partial muon-capture rate, then with our assumption of no second-class currents we have in principle four weak-

TABLE III. $0^+0 \leftrightarrow 1^+1$ transitions.

	Theoretical value ($b = 1.77$ F)	Experimental value	Amplitude reduction ξ
Electron scattering	(see Fig. 2)		2.25
γ-decay width	148 eV	36.68 ± 1.08 eV [a]	2.01 ± 0.03 [b]
β^--decay rate	171 sec^{-1}	32.98 ± 0.10 sec^{-1} [c]	2.28 ± 0.03 [b]
β^+-decay rate	339 sec^{-1}	59.55 ± 0.22 sec^{-1} [c]	2.38 ± 0.04 [b]
μ-capture rate	33.6×10^3 sec^{-1}	$6.75^{+0.30}_{-0.75} \times 10^3$ sec^{-1} [d]	$2.23^{+0.14}_{-0.05}$ [b]

[a] See B. T. Chertok, C. Sheffield, J. W. Lightbody, Jr., S. Penner, and D. Blum, to be published.
[b] Range obtained from experimental uncertainty.
[c] Including the branching ratios. See F. Ajzenberg-Selove and T. Lauritsen, Nucl. Phys. A114, 1 (1968).
[d] See E. J. Maier, R. M. Edelstein, and R. T. Siegel, Phys. Rev. 133, B663 (1964).

coupling constants at our disposal; F_1^V, μ^V, F_A, and $M_N F_P$. F_1^V is given by CVC (the muon-capture rate is very insensitive to F_1^V) and the $(\pi \to e + \nu)$ $(\pi \to \mu + \nu)$ branching ratio indicates that $F_A^\mu = F_A^\beta$. By fitting the inelastic electron scattering form factor we have no freedom in choosing μ^V for the weak processes, and yet as shown in Fig. 3, the agreement for the muon-capture rate between the calculated value using CVC and the experimental value is excellent. Moreover, the rate depends sensitively enough on the value of μ^V to show that for reasonably small deviations from CVC the agreement would be significantly worse. In the same figure the dependence on F_P is shown and we see that even for fairly large deviations from the pion-pole value the capture rate is relatively unchanged. This gives us a rather convincing demonstration of the presence of weak magnetism in muon capture, as has been pointed out previously.[1]

The classic demonstration of the presence of weak magnetism in β decay[8] is the experiment of Lee, Mo, and Wu[9] on the deviations of the $e^\pm$ spectra for reactions (57c) and (57d) from the allowed shape. Figure 4 shows a comparison of our calculated $e^\pm$ spectra [both normalized to 1 at $\epsilon = 5.45$ MeV] with the data of Ref. 9. Again, the present calculation uses the matrix elements of T_1^{mag} from electron scattering to determine b and ξ; there are then no free parameters in the calculation of the weak processes and the agreement between theory and experiment in Fig. 4 and Table III convincingly reaffirms the presence of weak magnetism in β decay for if μ^V were taken as zero in β decay, the two curves would be identical and essentially flat (recall that F_P makes no appreciable contribution to electron processes). The present theoretical calculation has the advantage of treating retardation correctly in the nuclear matrix elements and consistently evaluating the nuclear amplitudes in the leptonic processes up through order $(v/c)_{\text{nucleon}}$. It is interesting that this calculation introduces some curvature into the theoretical curves in Fig. 4; however, this curvature is evidently not significant at the present stage of comparison between theory and experiment.

B. Muon Capture and Neutrino Reactions in Mass 12

In this section we extend our study to include all the even- and odd-parity single-particle-hole $T = 1$ states studied previously in electron scattering. In the remainder of this work we shall use $b = 1.64$ F for the oscillator parameter as determined by the elastic electron scattering form factor. In accordance with the past work on inelastic electron scattering we shall require reduction factors of ~2 for the even-parity states (cf. Sec. III A) and $\sim\sqrt{2}$ for the odd-parity states. This is a rough rule of thumb for the actual reduction we would obtain using improved wave functions where the $1p$ shell was opened, and where backward- as well as forward-going amplitudes were permitted (RPA).[6] The actual single-particle-hole states used are given in Ref. 4.

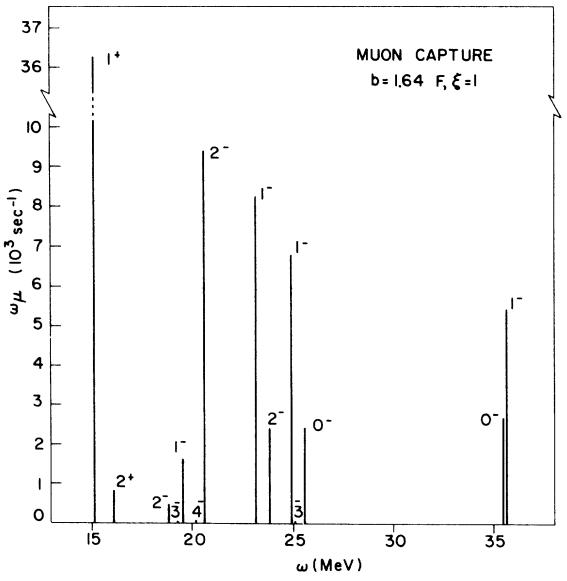

FIG. 5. Partial muon-capture rates. To compare with experiment the even-parity doublet should be reduced in amplitude by a factor $\xi \sim 2$ (a factor of 4 in the rates) and the odd-parity states should be reduced by $\xi \sim \sqrt{2}$ to produce agreement in electron scattering (see text).

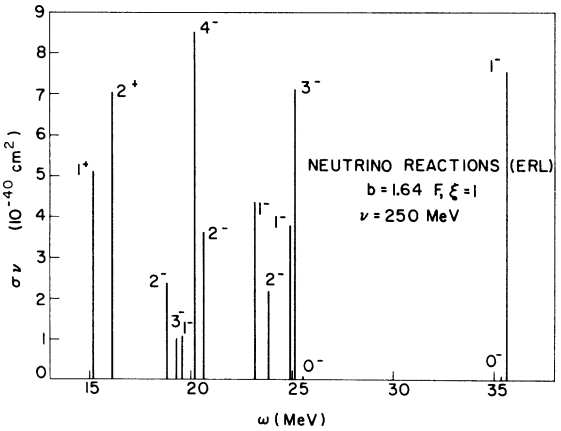

FIG. 6. Neutrino reactions in the extreme relativistic limit (ERL) at neutrino energy $\nu = 250$ MeV. For even- (odd-) parity states the amplitudes should be reduced by ~2 ($\sim\sqrt{2}$) to produce agreement in electron scattering (see text).

The unreduced partial muon-capture rates are shown in Fig. 5. We note in particular the dominance of the 1^+, 2^-, 1^-, and 0^- states, whereas the 2^+, 3^-, and 4^- states are relatively unimportant for muon capture. This should be contrasted with inelastic electron scattering, where at low momentum transfer the low multipolarity transitions dominate (except $0^+ \to 0^-$ which is forbidden in first Born approximation) while at medium to high values of momentum transfer the high spin states play a crucial role. For example the 4^- state dominates the inelastic electron scattering spectrum at momentum transfers around 300 MeV. The effective momentum transfer for muon capture on the other hand is in the range 70 to 90 MeV and in addition muon capture involves axial vector as well as vector-current matrix elements so that different aspects of the same nuclear wave functions are being explored. The total calculated capture rate with the reduction factors of 2 for even parity and $\sqrt{2}$ for odd parity is 29×10^3 sec^{-1}, to be compared with the experimental value[1] $36-39 \times 10^3$ sec^{-1}. The remaining strength unaccounted for here is presumably due to the excitation of states outside of the assumptions made in the present calculation, for example, states involving two or more major shells. An estimate of this strength (which is necessarily positive) is given by Foldy and Walecka[10] amounting to $\sim 5 \times 10^3$ sec^{-1} and brings the total calculated rate into essential agreement with experiment.

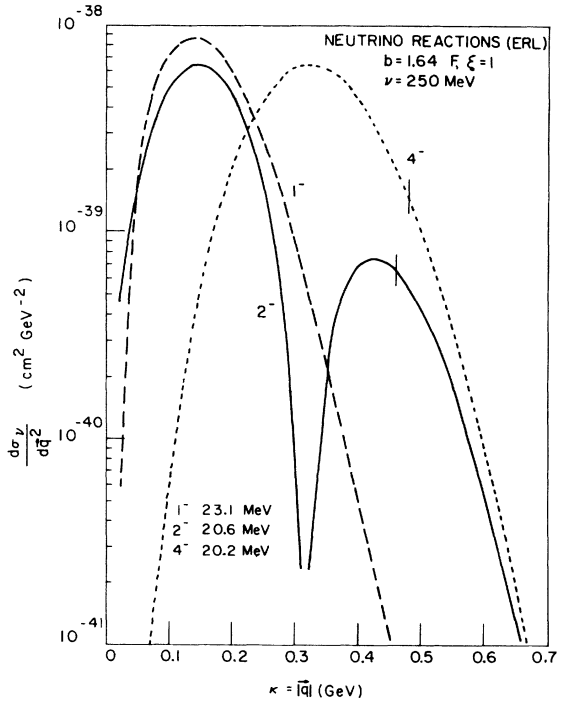

FIG. 7. Neutrino reaction cross sections (unreduced) as functions of momentum transfer $\kappa = |\vec{q}|$ at neutrino energy $\nu = 250$ MeV. The scattering angle θ varies with κ up to $\theta = 180°$, marked by vertical bars on the curves.

With the same wave functions we finally consider the neutrino reactions (57f) in mass 12.[11] In Fig. 6 we show the unreduced integrated partial cross sections as functions of the excitation energy ω for a neutrino energy of $\nu = 250$ MeV. These results are obtained in the ERL although the results obtained using the full kinematics only differ by a few percent at this neutrino energy. Thus the results apply equally to electron and muon neutrinos. However, once the muon-production threshold is approached the cross sections will differ, since there the ERL will still be valid for electrons, but not for muons. As in electron scattering, the neutrino reactions may involve higher values of momentum transfer than the other weak processes and again we find the high-multipolarity transitions playing a prominent part in determining the neutrino spectrum. This is a particularly interesting region of neutrino energies to be explored, since again we can learn more about the nuclear wave functions and about the electromagnetic and weak interactions themselves by comparing results from these various reactions.

In Fig. 7 we show the differential neutrino cross sections as functions of $\vec{q}^2$ for a few of the states which proved to be particularly important in electron scattering. These are not exactly the equivalent of electron scattering form factors, since the neutrino energy is held fixed at 250 MeV and as $\vec{q}^2$ varies the scattering angle θ also varies. In fact the upper limit where $\theta = 180°$ is indicated by a vertical bar on these curves. The behavior is similar to what has become familiar from inelastic electron scattering: at low momentum transfer the low multipoles dominate while at medium to high momentum transfer the high-spin states come into prominence.

To display the dependence on neutrino energy we show the total cross sections for all even- and all odd-parity states in Fig. 8. The solid lines marked electrons are essentially the ERL calculations, since the electron mass is so small. We see that at $\nu = 250$ MeV and higher the muon curves (dashed) differ only by a few precent from the ERL curves. These results are unreduced and for comparison with experiment (when available) should be multiplied by $1/\xi^2$, where $\xi \sim \sqrt{2}$ (odd-parity) or 2 (even-parity). The "asymptotic" total cross sections ($\nu = 20$ GeV) are indicated by arrows at the right of the figure. For all states of given parity taken together we show the unreduced differential cross sections in Fig. 9.

Since the first experiments with neutrinos to be

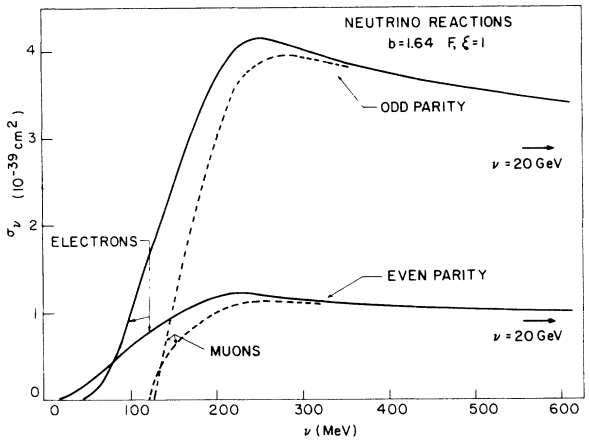

FIG. 8. Neutrino cross sections (unreduced) as functions of the neutrino energy ν for even- and odd-parity states. The predicted experimental cross sections are obtained by reducing the curves given here using amplitude reduction factors $\xi \sim 2$ and $\sim\sqrt{2}$ for even- and odd-parity states, respectively, to produce agreement with electron scattering (see text). For low ν the curves for electron and muon neutrino reactions differ, but merge in the extreme relativistic limit. The asymptotic cross sections (20 GeV) are indicated by arrows.

done at LAMPF[12] are to be for electron neutrinos at energies between 0 and 53 MeV obtained from the decay of stopped muons we also calculated the total neutrino cross section weighted with the electron neutrino spectrum and including the reduction factors for even- and odd-parity states. The theoretical result obtained is 1.46×10^{-41} cm^2. The peak in the weighted cross section occurs at about 45-MeV neutrino energy and at that point is made up from 72% even-parity and 28% odd-parity excitations (with reduction factors included). More

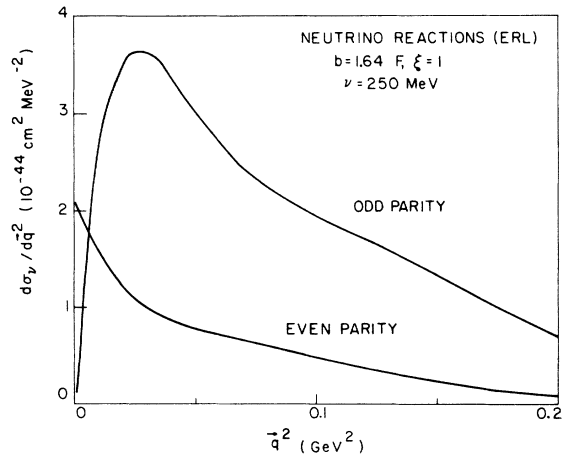

FIG. 9. Momentum transfer dependence of the (unreduced) neutrino cross sections at neutrino energy of ν = 250 MeV.

than 90% of the total weighted cross section comes from four states: the 1^+1 state (72%), the highest-lying 1^-1 state (4%), second highest-lying 1^-1 state (8%), and the 2^-1 giant quadrupole state near 20 MeV (9%).

IV. CONCLUSIONS

In the present work we have considered the semileptonic weak processes (β decay, μ capture, and neutrino reactions) and electromagnetic processes (γ decay and electron scattering) on a unified basis. The leptons involved are allowed to interact with the mass-12 nuclear system (B^{12}, C^{12}, N^{12}), where for the dynamics of the nuclear many-body problem we employ the single-particle-hole model.

We first consider inelastic electron scattering in detail to determine the matrix elements of the vector current in the electromagnetic case and by the CVC hypothesis take these matrix elements to be the same in the case of weak interactions. In addition, the comparison of calculated electron scattering form factors with experiment provides a stringent test of the nuclear wave functions involved. We proceed to use the *same* wave functions in studying the weak processes, where in addition to the vector current we must also deal with the axial-vector current. In principle the weak interactions provide us with a richer source of information on the nuclear many-body system. We find for example that the simple particle-hole model, with amplitudes reduced to give agreement in studying electron scattering form factors, gives essential agreement with all the weak interaction processes which have been investigated experimentally. Many interesting features seen in electron scattering such as the high-spin states also play a vital role in the weak reactions.

Once we have carried out such a unified analysis and have some confidence in our description of the nuclear system, we can proceed to say something about the interactions themselves: For example, we are able to make some meaningful statements about the coupling constants involved in the semileptonic weak interactions.

Finally, with some confidence as to the validity of both nuclear and particle aspects of the problem obtained in this unified treatment, we can proceed to calculate the cross sections for neutrino reactions where experimental data are not presently available.

ACKNOWLEDGMENTS

The first author would like to thank the Institute of Theoretical Physics, Stanford University, and the Aspen Center for Physics for their hospitality during the course of this work.

APPENDIX

In this Appendix we relate the neutrino cross section to the electron scattering form factors so that, under several assumptions which may be realized in practice, experimental electron scattering results can be used to predict neutrino cross sections. The cross section for the scattering of electrons of initial energy E_0 through angle θ with energy loss ω and three-momentum transfer $\kappa = |\vec{q}|$ is given by[2]

$$\frac{d\sigma_{ee'}}{d\Omega} = 4\pi\left[\frac{\alpha\cos\frac{1}{2}\theta}{2E_0\sin^2(\frac{1}{2}\theta)}\right]^2\left\{\left[\frac{q_\lambda^2}{\kappa^2}F_L^2(\kappa,\omega)\right] + \left[\frac{q_\lambda^2}{2\kappa^2}+\tan^2(\tfrac{1}{2}\theta)\right]F_T^2(\kappa,\omega)\right\}, \tag{A1}$$

where we neglect the center-of-mass, nucleon form factor, and recoil corrections. Here the longitudinal and transverse form factors are given by

$$F_L^2 = \frac{1}{2J_i+1}\sum_{J=0}^{\infty}|\langle J_f\|\hat{M}_J\|J_i\rangle|^2, \tag{A2}$$

$$F_T^2 = \frac{1}{2J_i+1}\sum_{J=1}^{\infty}\left(|\langle J_f\|\hat{T}^{\rm el}_J\|J_i\rangle|^2 + |\langle J_f\|\hat{T}^{\rm mag}_J\|J_i\rangle|^2\right). \tag{A3}$$

If the convection current part of the vector operators can be neglected [$\Delta_J^M = \Delta_J'^M = 0$, Eqs. (44), (45)], which is equivalent to the approximation that the nucleon velocity in the ground state is small [$(v/c)_{\rm nucleon} \ll 1$] then we can relate the electric and magnetic axial-vector and vector operators to one another [cf. Eqs. (37), (38), (41), (42)]:

$$\frac{2M_N}{\kappa\mu^V}T^{\rm el}_{JM} \simeq \Sigma''^M_J = \frac{1}{F_A}T^{{\rm mag}5}_{JM}, \tag{A4}$$

$$-\frac{i2M_N}{\kappa\mu^V}T^{\rm mag}_{JM} \simeq \Sigma'^M_J = -\frac{i}{F_A}T^{{\rm el}5}_{JM}. \tag{A5}$$

Then we find that for the weak processes

$$\frac{1}{2J_i+1}\sum_{J=1}^{\infty}\left(|\langle J_f\|\hat{T}^{\rm el}_J\|J_i\rangle|^2 + |\langle J_f\|\hat{T}^{\rm mag}_J\|J_i\rangle|^2\right) \simeq \left[1+\left(\frac{2M_NF_A}{\kappa\mu^V}\right)^2\right]F_T^2 \tag{A6}$$

and

$$\frac{1}{2J_i+1}\sum_{J=1}^{\infty}{\rm Re}\langle J_f\|\hat{T}^{\rm mag}_J\|J_i\rangle\langle J_f\|\hat{T}^{\rm el}_J\|J_i\rangle^* \simeq \frac{2M_NF_A}{\kappa\mu^V}F_T^2 \tag{A7}$$

for states of either parity. The longitudinal vector operators for the neutrino reactions in ERL may be directly related to the longitudinal electron scattering form factor

$$\frac{1}{2J_i+1}\sum_{J=0}^{\infty}|\langle J_f\|\hat{M}_J + \frac{\omega}{\kappa}\hat{L}_J\|J_i\rangle|^2 = \left(\frac{q_\lambda^2}{\kappa^2}\right)^2\frac{1}{2J_i+1}\sum_{J=0}^{\infty}|\langle J_f\|\hat{M}_J\|J_i\rangle|^2 = \left(\frac{q_\lambda^2}{\kappa^2}\right)^2F_L^2, \tag{A8}$$

while we have for the axial-vector operators in ERL neglecting the operator Ω_J^M [Eq. (49)] whose contribution is small if $(v/c)_{\rm nucleon} \ll 1$:

$$\frac{1}{2J_i+1}\sum_{J=0}^{\infty}|\langle J_f\|\hat{M}^5_J + \frac{\omega}{\kappa}\hat{L}^5_J\|J_i\rangle|^2 \simeq \left(\frac{\kappa}{2M_N}-\frac{\omega}{\kappa}\right)^2\sum_{J=0}^{\infty}|\langle J_f\|F_A\hat{\Sigma}''^M_J\|J_i\rangle|^2. \tag{A9}$$

These matrix elements multiplied by $\cos^2(\frac{1}{2}\theta)$ [Eq. (25)] compete with the matrix elements involving $T^{{\rm el}5}_{JM}$ which involve $F_A\hat{\Sigma}'^M_J$, but with kinematic factor $(q_\lambda^2/2\kappa^2)\cos^2(\frac{1}{2}\theta)+\sin^2(\frac{1}{2}\theta)$. Since the matrix elements of the spin multipoles are of the same order of magnitude and we have

$$\left(\frac{\kappa}{2M_N}-\frac{\omega}{\kappa}\right)^2\cos^2(\tfrac{1}{2}\theta) \ll \frac{q_\lambda^2}{2\kappa^2}\cos^2(\tfrac{1}{2}\theta)+\sin^2(\tfrac{1}{2}\theta)$$

in a large region of interest, i.e., except in the very forward direction, we may then to a good approximation neglect the longitudinal axial-vector contributions altogether. The final result for the neutrino cross

sections in ERL is, using Eq. (12),

$$\left(\frac{d\sigma_{\nu}}{d\vec{q}^2}\right)^{\mathrm{ERL}}_{\substack{\nu\\ \bar{\nu}}} \simeq 2G^2\left(\frac{\epsilon}{\nu}\right) 2(T+1)\cos^2(\tfrac{1}{2}\theta)\Bigg(\left[\frac{q_\lambda{}^2}{\kappa^2}\right]^2 F_L{}^2(\kappa,\omega) + \left\{\left[\frac{q_\lambda{}^2}{2\kappa^2}+\tan^2(\tfrac{1}{2}\theta)\right]\left[1+\left(\frac{2M_N}{\kappa\mu^V}F_A\right)^2\right] \mp \tan(\tfrac{1}{2}\theta)\left[\frac{q_\lambda{}^2}{\kappa^2}+\tan^2(\tfrac{1}{2}\theta)\right]^{1/2}\frac{4M_N}{\kappa\mu^V}F_A\right\} F_T{}^2(\kappa,\omega)\Bigg). \tag{A10}$$

As long as the momentum transfer and scattering angle are large enough so that in electron scattering the isoscalar contributions may safely be neglected with respect to the isovector contributions, but not so large that the longitudinal axial-vector contributions can compete with the transverse axial-vector electric contribution, this is a useful relationship for predicting neutrino cross sections using the electron scattering inelastic form factors.

---

†Research sponsored in part by the Air Force Office of Scientific Research, Office of Aerospace Research, U. S. Air Force, under AFOSR Contract No. F44620-71-C0044.

*This work was initiated while the first author was a visitor at the Institute of Theoretical Physics, Stanford University, 1970–71. A preliminary version of these results was reported in Ref. 1 and by J. S. O'Connell, Bull. Am. Phys. Soc. 17, 58 (1972).

[1]J. D. Walecka, in Muon Physics, edited by V. W. Hughes and C. S. Wu (Academic, N.Y., to be published).

[2]T. deForest, Jr., and J. D. Walecka, Advan. Phys. 15, 1 (1966).

[3]T. W. Donnelly, J. D. Walecka, I. Sick, and E. B. Hughes, Phys. Rev. Letters 21, 1196 (1968).

[4]T. W. Donnelly, Phys. Rev. C 1, 833 (1970).

[5]We take $\hbar=c=1$ and denote four vectors by $k_\lambda=(\vec{k}, ik_0)$, where $k_\lambda{}^2=\vec{k}^2-k_0{}^2$. The summation convention over repeated indices $\lambda=1, 2, 3, 4$ is employed.

[6]T. W. Donnelly, D. J. Rowe, and S. S. M. Wong, to be published.

[7]D. Kurath, Phys. Rev. 134, B1025 (1964).

[8]M. Gell-Mann, Phys. Rev. 111, 362 (1958).

[9]Y. K. Lee, L. W. Mo, and C. S. Wu, Phys. Rev. Letters 10, 253 (1963).

[10]L. L. Foldy and J. D. Walecka, Nuovo Cimento 34, 1026 (1964).

[11]There is a previous calculation of neutrino cross sections within the framework of the particle-hole model in which only the 0^-, 1^-, and 2^- states are considered [see F. J. Kelly and H. Überall, Phys. Rev. 158, 987 (1967)]. Our numerical results are in general agreement with theirs, but there is significant disagreement for a few individual states. As the present calculations have been checked independently, we believe the present results. In addition, we have used these same wave functions in a detailed comparison with electron scattering to estimate the validity of the present neutrino reaction calculations. Furthermore, it is essential to include the high-spin particle-hole states, as they can make a significant contribution to the cross section (see Fig. 6).

[12]Los Alamos Scientific Laboratory Report No. LA-4842-MS, 1971 (unpublished).